

Earth's Future

RESEARCH ARTICLE

10.1029/2025EF006516

Key Points:

- Anthropogenic aerosols have masked the heatwave intensifications in duration and cumulative heat from the industrial era
- Recent reductions in aerosols exacerbate heatwave intensifications rates exceeding those attributable to greenhouse gases alone
- Diminishing aerosol forcing has driven significant changes in cloud cover and shortwave radiation at regional scale

Supporting Information:

Supporting Information may be found in the online version of this article.

Correspondence to:

W. Wang,
wangweiguang@hhu.edu.cn

Citation:

Wei, J., Wang, W., Teuling, A. J., Zhang, J., Wang, G., Jin, J., et al. (2025). Reduced anthropogenic aerosols reveal increased heatwaves driven by climate warming. *Earth's Future*, 13, e2025EF006516. <https://doi.org/10.1029/2025EF006516>

Received 20 APR 2025

Accepted 15 JUN 2025






Author Contributions:

Conceptualization: Weiguang Wang
Investigation: Jia Wei, Weiguang Wang, Jianyun Zhang, Guoqing Wang, Junliang Jin, Xiaoyin Liu, Mingzhu Cao, Hongbin Li, Liyan Yang
Methodology: Jia Wei, Weiguang Wang, Adriaan J. Teuling, Jianyun Zhang, Guoqing Wang
Supervision: Weiguang Wang
Visualization: Jia Wei, Weiguang Wang, Jianyun Zhang, Guoqing Wang, Junliang Jin, Xiaoyin Liu, Mingzhu Cao
Writing – original draft: Jia Wei
Writing – review & editing: Weiguang Wang, Adriaan J. Teuling, Jianyun Zhang, Guoqing Wang, Junliang Jin, Xiaoyin Liu, Mingzhu Cao, Hongbin Li, Liyan Yang, Shuo Wang

© 2025. The Author(s).

This is an open access article under the terms of the [Creative Commons Attribution License](https://creativecommons.org/licenses/by/4.0/), which permits use, distribution and reproduction in any medium, provided the original work is properly cited.

Reduced Anthropogenic Aerosols Reveal Increased Heatwaves Driven by Climate Warming

Jia Wei^{1,2,3}, Weiguang Wang^{1,2,4} , Adriaan J. Teuling⁵ , Jianyun Zhang^{1,2,4,6}, Guoqing Wang^{1,2,4,6} , Junliang Jin^{1,4} , Xiaoyin Liu^{1,7}, Mingzhu Cao^{1,2}, Hongbin Li^{1,2}, Liyan Yang^{1,2}, and Shuo Wang³ 

¹National Key Laboratory of Water Disaster Prevention, Hohai University, Nanjing, China, ²College of Hydrology and Water Resources, Hohai University, Nanjing, China, ³Department of Land Surveying and Geo-Informatics, Research Institute for Sustainable Urban Development, The Hong Kong Polytechnic University, Hong Kong, China, ⁴Yangtze Institute for Conservation and Development, Hohai University, Nanjing, China, ⁵Hydrology and Quantitative Water Management Group, Wageningen University, Wageningen, The Netherlands, ⁶Nanjing Hydraulic Research Institute, Nanjing, China, ⁷College of Agricultural Science and Engineering, Hohai University, Nanjing, China

Abstract Understanding the contributions of anthropogenic climate forcings to heatwave intensification is essential for evaluating mitigation strategies. While greenhouse gas influences on temperature extremes are well established, the impacts of other anthropogenic forcings, particularly aerosols, remain inadequately characterized. Here, we quantify the distinct contributions of greenhouse gases, anthropogenic aerosols, and natural forcings to extreme heatwave metrics from the pre-industrial period. Globally, changes in the duration of heatwave events and cumulative heat are $+2.77 \pm 0.85$ days and $+1.76 \pm 0.31^\circ\text{C}^2$ attributed to greenhouse gases, and -1.10 ± 0.34 days and $-0.85 \pm 0.14^\circ\text{C}^2$ due to anthropogenic aerosols, respectively, over the past 3 decades relative to pre-industrial levels. This indicates that aerosols substantially masked greenhouse gas effects until the 1990s. Under current mitigation policies, declining aerosol emissions have exacerbated heatwave intensification at rates of $+1.07 \pm 0.32$ days decade⁻¹ and $+0.47 \pm 0.09^\circ\text{C}^2$ decade⁻¹ for duration and cumulative heat respectively, exceeding the intensification attributable to greenhouse gases alone. Heatwave intensification has been driven primarily by reduced cloud cover and increased shortwave radiation resulting from weakening aerosol forcing, especially in Central North America and Europe. However, the regional climate changes driven by greenhouse gases and aerosols exhibit spatial heterogeneity, highlighting the necessity for geographically targeted mitigation strategies.

Plain Language Summary The commitment of parties to the Paris Agreement includes efforts to limit the increase in global temperature above pre-industrial levels. Understanding the contributions of human-induced climate forcings to hot extremes is crucial for assessing our progress toward these goals. Until the 1990s, aerosols significantly masked the greenhouse gas effect, resulting in an acceleration of 1.07 ± 0.32 days per decade and $0.47 \pm 0.09^\circ\text{C}^2$ per decade for heatwave duration and cumulative heat, respectively. These rates exceed the increases driven solely by greenhouse gases. With the efforts of climate change mitigation policies, inadvertent decreases in aerosols unmask their cooling effects and contribute to net warming, playing an important role in regional heatwaves. These increases surpass the intensifications caused by anthropogenic greenhouse gases alone. Central Northern America and Europe have experienced heatwave intensifications driven by the reduction in cloud cover and increase in shortwave radiation induced by weakening anthropogenic aerosols. However, the divergent contributions of greenhouse gases and aerosols to regional climate exhibit spatial differences, highlighting the urgent need for targeted actions in key geographical regions.

1. Introduction

As one of the most impactful natural hazards, heatwaves have caused extensive detrimental impacts on ecosystems and societies across the globe (Allen et al., 2015; Bras et al., 2021; Teuling et al., 2010; Wei, Han, et al., 2023). Unlike individual hot days, heatwave events last over a span of days, significantly escalating risks of wildfire and substantial morbidity and mortality (Åström et al., 2013; Guo et al., 2018; Lobell & Field, 2007; Teuling, 2018; Westerling et al., 2006; Xu et al., 2016). Historically, heatwave and induced drought resulted in €15 billion loss in Europe in 2003 while 32.8 billion CNY in the Yangtze River basin in 2022 summer (Tang et al., 2023; Tripathy & Mishra, 2023). Particularly, the progressive intensification of extreme heatwaves imposes

irreversible changes of ecosystem, pushing numerous organisms and ecosystems to the limits of resilience (Ciais et al., 2005; Smale et al., 2019). Considerable efforts have gone into reaching the Paris Agreement goals to constrain human influences on global temperature increases relative to pre-industrial levels (Schurer et al., 2017; UNFCCC, 2015). Even so, anthropogenic emissions have caused $\sim 1.0^{\circ}\text{C}$ of warming in global mean temperature in recent decades relative to the pre-industrial period (Barkhordarian, 2024; Diffenbaugh et al., 2017; Gillett et al., 2021; Kim et al., 2016; Padrón et al., 2020). While the central role of greenhouse gases in increasing temperature is well understood, only a few studies have focused on the influences of other anthropogenic forcings, such as aerosols, on heatwaves and the global distribution of their net impacts.

Quantification of the impacts of human-induced climate forcings to extreme heatwaves is not straightforward, particularly for anthropogenic aerosols. Generally, aerosols have a cooling effect through their interacting with radiation and clouds, thus masking the total global warming (Bellouin et al., 2020; Meinshausen et al., 2009). However, the magnitude of the aerosol impact is highly uncertain due to the complexity of aerosol composition and their shorter lifecycles compared to greenhouse gases (Mhawish et al., 2022; Wild et al., 2005). While greenhouse gases are generally well-mixed in the atmosphere, anthropogenic aerosols have more distinct emission sources, which in combination with the short lifecycle results in high spatial heterogeneity across the globe over the industrial era (Nair et al., 2023; Persad & Caldeira, 2018; Tan et al., 2023; Wang et al., 2024). The aerosols distribute extensively in regions experienced heavy pollution and intensive human activities, which are located with monsoon system (Li et al., 2016; Zhang et al., 2012). Under ongoing climate change mitigation policies, reducing emissions will also decrease co-emitted aerosols, potentially demasking their cooling effects and contributing to net warming, which is important for understanding the impacts of human actions on regional environment and their implications for extreme events (Chemke & Yuval, 2023; Grant et al., 2021). For example, combined effects of air pollution control measures and continued greenhouse gases emissions changed precipitation regimes from dipolar to monopolar in the high mountains of Asia (Jiang et al., 2023). However, with international attention and cooperative solutions on targeting emissions, the consequence of global mitigation on heatwave evolutions is little known. The combined impacts of reduced long-lived greenhouse gases and shorter-lived anthropogenic aerosols on heatwaves in the industrial era remain unclear. While identifying the individual anthropogenic forcing effects is challenging (Marvel et al., 2019; Padrón et al., 2020), state-of-the-art climate models enable a global estimation of human-induced climate forcings to heatwaves from the pre-industrial period, which is crucial for monitoring progress toward the Paris Agreement goals and understanding the sustainability of current mitigation policies.

Here, we present a global assessment of the impacts of anthropogenic and natural forcings on changes in multifaceted heatwave characteristics worldwide. We use four observational data sets and the Coupled Model Intercomparison Project Phase 6 (CMIP6) climate model historical simulations to derive the modified excess heat factor (EHF) as influenced by anthropogenic and natural forcings. The modified EHF framework analyzes heatwave events from 1850 to 2021, considering both local heat anomalies and temperature thresholds. Heatwave evolutions are initially analyzed using available observations. Further, the Detection and Attribution Model Intercomparison Project (DAMIP) scenarios—greenhouse gases-only, anthropogenic aerosols-only and natural-only—are used to assess each individual forcing contributions. Additionally, the impacts of human-induced forcings on cloud and radiation changes are quantified for each anthropogenic forcing. Using 24 CMIP6 climate model ensemble members of four climate forcing scenarios, we quantify changes in extreme heatwave duration and cumulative heat attributable to each anthropogenic and natural forcing since the pre-industrial era. The SSP2-4.5 scenario for 2015–2020 is employed to merge with historical simulations (1850–2014) to ensure consistency over the examined period (1850–2020). Our findings have significant implications for the development of climate change mitigation policies and human interventions to address increasing heatwave risks in key geographical regions.

2. Materials and Methods

2.1. Data

We use temperature data from ERA5 (1940–2022), JRA55 (1958–2022), MERRA2 (1980–2022), and NCEP/NCAR (1948–2022), which are first averaged to a daily scale. The examined period is as long as the availability of each data set. The daily temperatures from historical simulations (1850–2014) of 24 climate model ensemble members in the CMIP6 (Eyring et al., 2016) are also used, which include all anthropogenic forcings and natural

forcings to reflect historical temperature variations. In order to explore the contributions of human-induced emissions on heatwave changes, we utilize simulations from the DAMIP spanning 1850–2020. These include historical runs driven solely by greenhouse gases (GHG-only), by anthropogenic aerosols (AA-only), and by natural factors (NAT-only), which allow us to examine individual anthropogenic forcings of greenhouse gases and anthropogenic aerosols (Gillett et al., 2016). In addition, we obtain daily temperatures from the ScenarioMIP SSP2-4.5 simulations to extend CMIP6 historical simulations from 2014 to 2020. Each individual historical CMIP6 simulations (1850–2014) was merged with SSP2-4.5 simulations for 2015–2020 to ensure consistency. The SSP2-4.5 simulations have moderate level of greenhouse gas emissions and a broad range of SSP-based integrated assessment models (Gillett et al., 2021; O'Neill et al., 2016). The 2020 endpoint enables comparisons between CMIP6 historical and DAMIP simulations, which is consistent with Tier 1 experiments of DAMIP methodology (Gillett et al., 2016). The detailed information of each climate model can be found in Table S1 of Supporting Information S1. Finally, for comparison with the consistent resolution at a global scale, observations and simulations are regridded to a regular resolution of $1^\circ \times 1^\circ$ using bilinear interpolation across all land areas.

2.2. Modified Heatwave Definition

The common heatwave definitions usually use a threshold of extreme temperature such as 90th or 95th percentile of maximum and minimum temperatures to identify excessive heat during day and night (e.g., Fischer & Schär, 2010; Mukherjee & Mishra, 2021; Russo et al., 2015; Sharma & Mujumdar, 2017; Wei et al., 2020, 2023b; White et al., 2013; Zhu et al., 2022). However, daily temperatures have large differences across the globe affected by latitude, topography, and climate zones, resulting in diverse heatwave definitions with specific study region or purpose. Obviously, absolute temperature thresholds of heatwave are difficult to apply on a global scale. The relative temperature thresholds reach their limit in cold regions, where people no longer experience statistically hot extremes. Identifying the changes in heatwaves relative to the pre-industrial period at a global scale has been hindered by the numerous ways. Here, we propose a comprehensive and consistent metric to establish a consensus on the duration and cumulative heat of heatwave events. We initially utilize the excess heat factor (EHF) to evaluate the excess heat and heat stress. The EHF considers both the thermal stress exceeding the system's capacity and the impact of short-term heat exposure, offering a thorough assessment of heatwave characteristics worldwide. Currently, the EHF has been extensively tested for reliably detecting heatwave events (Nairn et al., 2018; Nairn & Fawcett, 2015; Perkins et al., 2012, 2015). However, in the high latitude regions such as Greenland, no detrimental impact of statistically high temperatures can be expected, leading to an overestimation of heatwaves based on such relative temperature criteria. Thus, we introduced a specific temperature threshold of 25°C into the relative temperature threshold framework of EHF to better investigate the heatwave characteristics on a global scale. The EHF framework contains two parts: excess heat and heat stress. The excess heat (EHI_{sig}) measures unusual high heat over a 3-day period, arising from high daytime heat which cannot sufficiently discharge overnight. For meteorological terms, the 3-day temperature is used to characterize the accumulated heat load leading to excess heat. This average 3-day temperature is compared against the climate reference value to express the long-term temperature anomaly:

$$\text{EHI}_{\text{sig}} = (T_i + T_{i-1} + T_{i-2})/3 - T_{i95}, \quad (1)$$

$$(T_i + T_{i-1} + T_{i-2})/3 \geq 25^\circ\text{C} \quad (2)$$

T_i is daily temperature derived from climate model simulations and the average temperature from the four observational data sets. The 95th percentile (T_{i95}) is calculated for each day (i) with a 15-day window (from T_{i-7} to T_{i+7}) centered on T_i for the period of data availability with 1940–2022, 1958–2022, 1980–2022 and 1948–2022 for the ERA5, JRA55, MERRA2 and NCEP/NCAR, respectively.

The heat stress (EHI_{accl}) represents the 3-day temperature anomaly against the local acclimatization during the recent past. The acclimatization of physical adaptation to hot temperatures usually takes 2–6 weeks since both biological and engineered systems require an adaptive response (Nairn et al., 2013). In the EHF framework, 30 days is used as the required period for acclimatization:

$$\text{EHI}_{\text{accl}} = (T_i + T_{i-1} + T_{i-2})/3 - (T_{i-3} + \dots + T_{i-32})/30, \quad (3)$$

$$(T_i + T_{i-1} + T_{i-2})/3 \geq 25^\circ\text{C} \quad (4)$$

The combined effect of excess heat and heat stress (EHF) is used to characterize hot extremes with respect to the local climate:

$$\text{EHF} = \text{EHI}_{\text{sig}} \times \max(1, \text{EHI}_{\text{acc}}), \quad (5)$$

Heatwave condition exists when the EHF is positive.

In our analysis, a heatwave event is detected with $\text{EHF} > 0$ for at least three consecutive days. Further, the duration of heatwave events is identified as the total participating days in a heatwave event (Wei et al., 2020, 2023b). For climate model simulations, heatwave events are calculated for the extended summer during the period 1850–2020 (May–September in the Northern Hemisphere, November–March in the Southern Hemisphere). For the observational data sets, it is calculated for the period of data availability with 1940–2022, 1958–2022, 1980–2022 and 1948–2022 for the ERA5, JRA55, MERRA2 and NCEP/NCAR, respectively.

The heatwave events are first calculated at each grid box level. For a regional scale, we selected the regions used in the IPCC Assessment Report SREX regions. Heatwave characteristics are spatially averaged according to each SREX region. By introducing the specific absolute temperature in the EHF calculation framework, the statistical heat extremes in cold regions are filtered. For example, the heatwave events in the Alaska, Greenland, Tibetan Plateau, and West Coast South America are eliminated using the new EHF method.

2.3. Cumulative Heat of Heatwave Events

The cumulative heat describes the extra heat load during heatwave events, which is affected by the duration and intensity of a heatwave event. The cumulative heat exposure (heat_{cum}) expresses total EHF values of heatwaves based on the calculation framework of EHF:

$$\text{heat}_{\text{cum}} = \sum_1^n \text{EHF} \quad (6)$$

where n is the duration of a heatwave event. The calculation framework of EHF is consistent with the modified heatwave definition section. For each grid box, we calculate the averaged cumulative heat (HWC) during a heatwave event:

$$\text{HWC} = \text{heat}_{\text{cum}}/\text{HWD} \quad (7)$$

where HWD is the total days of a heatwave event.

Unlike the duration of heatwaves, the cumulative heat provides the assessment of heat anomaly exceeding extreme thresholds, which can avoid overestimation of inflating heat exposure by summing absolute temperature anomalies during heatwaves. We calculated average cumulative heat as excess heat during heatwaves to better assess the sustained heat anomalies exceeding local thresholds. High-HWC values indicate severe impacts that arise from the averaged cumulative heat of a heatwave event.

2.4. Statistical Analysis

Decadal trends are calculated using Sen's Kendal slope method for each land grid cell, with the confidence level of 95%. Decadal trends are firstly calculated for the entire study period of 1851–2019. Compared to the pre-industrial period, the evolutions of heatwave duration and cumulative heat show significant shifts in recent decades. This indicates that trends of the entire study period cannot describe real changes across different stages from the pre-industrial period. Therefore, we examine the changes in decadal trends by commencing each year from 1851 to 1990, that is, the decadal trends are calculated from 1851–2019 to 1990–2019 with the 1-year moving window. The commencing year ends in 1990 to make the study period at least of 30 years, since a robust assessment of heatwave changes is recommended using a period of 3–4 decades for averaging temperature trends (Marotzke & Forster, 2015; Perkins & Lewis, 2020). Decadal trends are also calculated at each land grid cell and spatially averaged according to the IPCC SREX regions at a regional scale.

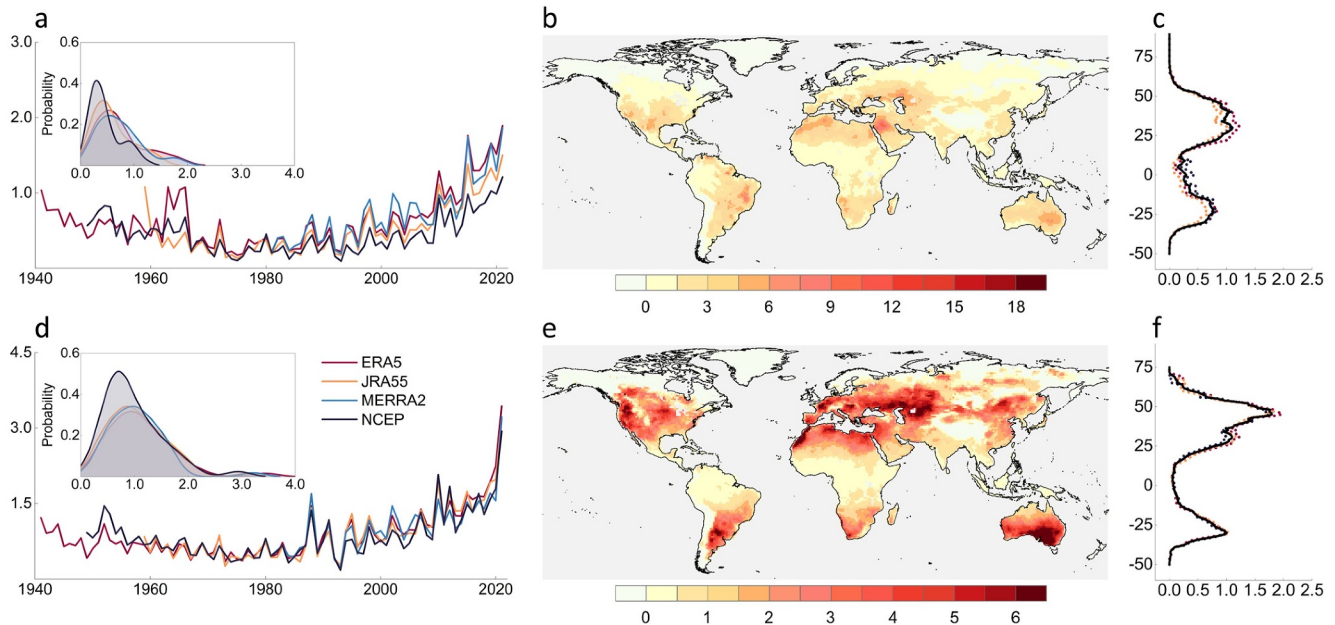


Figure 1. Changes in observed heatwave characteristics during the historical period. (a) Time series of the duration (days) in extreme heatwave events calculated from ERA5, JRA55, MERRA2 and NCEP/NCAR data sets, respectively. The probability distributions of the heatwave duration from these four data sets are shown in the upper left panel. (b) Global pattern of the duration in extreme heatwave events during recent decades (2002–2021). Heatwave characteristics are identified at each grid cell for each data set and are then averaged with consideration of the weights of grid areas. (c) Average latitudinal changes of the duration in extreme heatwave events. The solid black line shows the mean value of the four data sets. (d–f) Same as (a–c) but for the daily average cumulative heat ($^{\circ}\text{C}^2$) during the extreme heatwave events.

We extend the PR framework to assess changes in heatwave trends. We analyze the heat risks in the past decades (1990–2019) through the calculation of the probability ratios (PR) of the heatwave trend using the duration and cumulative heat of heatwave events from the historical observations, historical GHG-only, and AA-only simulations. The PR metric is referred to as a risk ratio in previous studies (Stott et al., 2004; Thiery et al., 2020; van der Wiel & Bintanja, 2021; Zhang et al., 2023). Here, we use PR metric to examine the risk ratio of anthropogenic forcings compared to observational heatwave changes, which can provide common understanding of the impacts of the greenhouse gases, anthropogenic aerosols on heatwave intensification. All PR values are calculated at each land grid cell and are spatially averaged over the IPCC SREX regions.

The PR of each grid box is defined as:

$$\text{PR} = \frac{P_{\text{hist-ANT}}}{P_{\text{hist-obs}}} \quad (8)$$

where $P_{\text{hist-ANT}}$ represents the probability of the heatwave duration and the cumulative heat occurring in the GHG-only and AA-only simulations, respectively. $P_{\text{hist-obs}}$ represents the probability of heatwave duration and cumulative heat from the observations.

3. Results

3.1. Evolution of Extreme Heatwaves

Definitions of heatwave events in existing literature are inconsistent due to significant temperature variations across the globe. In this study, we identify extreme heatwave events based on a modified EHF framework. Global evolutions of heatwave duration and cumulative heat calculated using different daily temperature data sets are shown in Figure 1. The heatwave duration indicates the number of extreme hot days during a heatwave event, while the cumulative heat reflects the heat exposure associated with the heatwave intensity. Thus, the modified EHF framework provides more comprehensive information than traditional heatwave metrics. Significant increases in these heatwave characteristics are detected in all data sets (ERA5, JRA55, MERRA2 and NCEP/NCAR) with high consistency (Figures 1a and 1d). However, the heatwave duration calculated from NCEP/

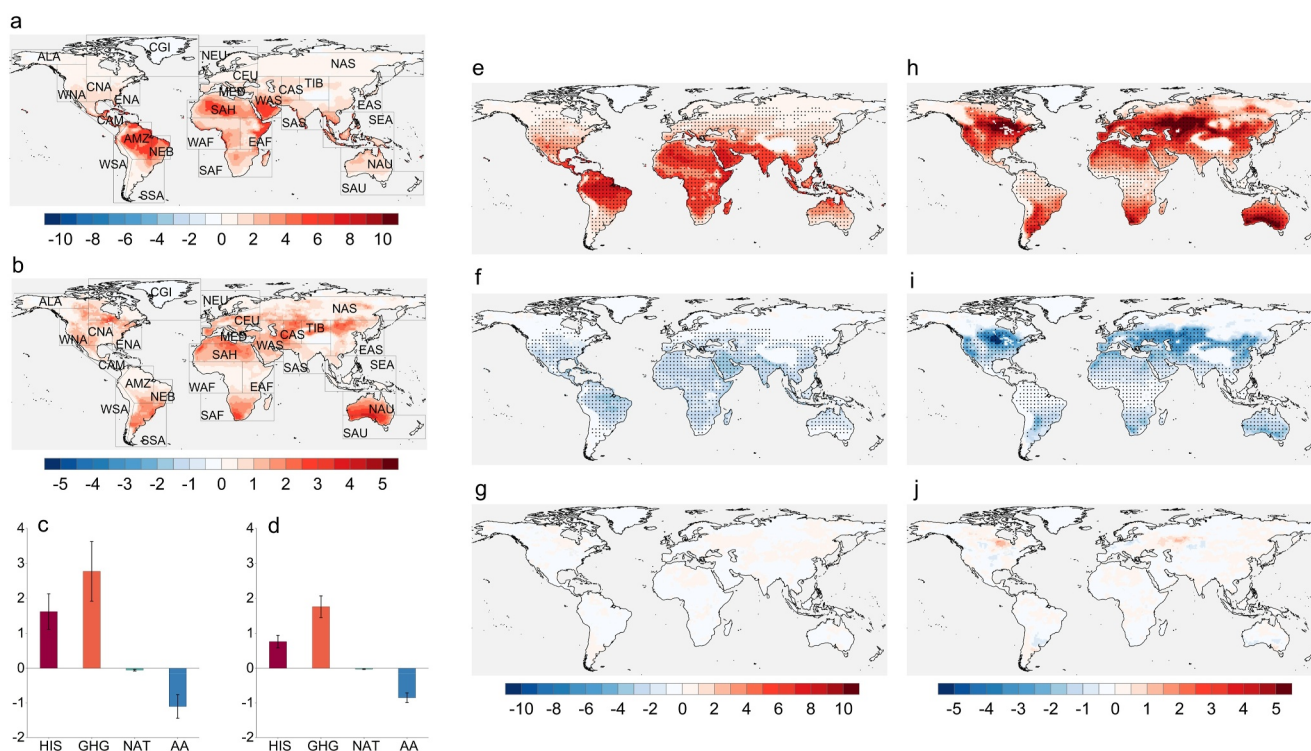


Figure 2. Global shifts in heatwave characteristics from the historical, greenhouse gas-only, anthropogenic aerosol-only, and natural-only simulations. (a) Spatial patterns of the difference in the duration of heatwave events between recent 3 decades (1990–2019) and pre-industrial period (1851–1880) from CMIP6 historical simulations. (b) Same as (a) but for the daily average cumulative heat during the extreme heatwave events. The IPCC SREX regions are indicated. (c, d) Differences in the duration and daily average cumulative heat between the 1990–2019 and 1851–1880 are averaged with consideration of the weights of grid areas under historical, greenhouse gas-only, anthropogenic aerosol-only, and natural-only conditions. Error bars indicate the standard deviation of 24 climate model ensembles. (e, f) Spatial patterns of the differences between the 1990–2019 and 1851–1880 in the extreme heatwave duration under greenhouse gas-only, anthropogenic aerosol-only, and natural-only forcings. (h–j), same as (e, f) but for the daily average cumulative heat during the extreme heatwave events. Dotted regions indicate the differences are significant at 0.05 statistical significance level.

NCAR is slightly lower than in other data sets. In recent decades, the heatwave duration and cumulative heat exhibit heterogeneous patterns. Longer heatwaves are observed in Europe, northern Africa, southern North America, eastern South America and Australia (Figure 1b). The heatwave duration is longer in the mid-latitudes of the Northern Hemisphere compared to the Southern Hemisphere (Figure 1c). On the other hand, the global cumulative heat of heatwave events has significantly increased, particularly in the mid-latitudes such as northern Asia, southern South America and southern Australia (Figure 1e). The peak value of cumulative heat is found in higher latitudinal regions than the heatwave duration. For example, although eastern Australia experiences longer heatwaves, the heat exposure is more severe in southern Australia (Figures 1e and 1f). These results indicate that the areas vulnerable to intense heatwaves differ from those exposed to longer heatwaves. The anthropogenic factors driving these intensifications and their geographical patterns require further investigation.

3.2. Contributions of Human-Induced Climate Change

We first analyze the global increases in heatwave duration and cumulative heat calculated from CMIP6 historical simulations. The historical simulations (1850–2014) are merged with SSP2-4.5 simulations (2015–2020) to ensure consistency with the simulations from the DAMIP scenarios. Globally, the duration of heatwave events in the past 3 decades (1990–2019) has increased by a factor of 5.12 compared to the pre-industrial period (1851–1880), with significant distribution in mid-lower latitude regions (Figures 2a and 2c). Compared to the pre-industrial period, the cumulative heat has increased by a factor of 1.76 times distributed extensively in mid-latitude regions (Figures 2b and 2d). Overall, heatwave changes driven by greenhouse gas-only (GHG-only) and anthropogenic aerosol-only (AA-only) forcings show opposite trends, while natural climate forcings (NAT-only) have negligible contributions to the heatwave intensification (Figure 2 and Figure S1 in Supporting

Information S1). Compared to the pre-industrial period, greenhouse gas simulations show positive impacts on heatwave duration and cumulative heat, with increases of $+2.77 \pm 0.85$ days and $+1.76 \pm 0.31^\circ\text{C}^2$, respectively. In contrary, anthropogenic aerosol simulations show decreases in these heatwave characteristics, with reductions of -1.10 ± 0.34 days and $-0.85 \pm 0.14^\circ\text{C}^2$, respectively. The increase ratios of heatwave duration and cumulative heat driven by GHG-only forcing are 1.71 and 2.30 compared to historical simulations, while the decrease ratios driven by AA-only forcing are -0.68 and -1.11 . These results indicate that the cooling effects of anthropogenic aerosols have a greater influence on heatwave intensity rather than duration. Furthermore, spatial distributions of the differences in these heatwave characteristics between 1990–2019 and 1851–1880 indicate that contributions of individual anthropogenic forcings to cumulative heat exhibit significant global heterogeneity.

Except for regions where the average 3-day temperature falls below 25°C , such as CGI, ALA, TIB and WSA, other regions, including Africa and South America, experience longer heatwave events, while North America and Europe endure stronger heatwaves. Asia experiences both longer and stronger heatwaves. We further analyze regional changes using the IPCC Assessment Report: Special Report on Managing the Risks of Extreme Events and Disasters to Advance Climate Change Adaptation (SREX) regions (Table S2 in Supporting Information S1). On regional scales, the impacts of greenhouse gases and anthropogenic aerosols show significant differences in heatwave properties. For instance, enhanced increases in heatwave duration driven by GHG-only forcing are larger in AMZ and NEB, while its effects on cumulative heat are strongest in SSA (Figures S2 and S3 in Supporting Information S1). A similar signal is observed in SAU and CEU. The mitigated effects of anthropogenic aerosols also show significant regional differences. While anthropogenic aerosols have a greater impact on reducing cumulative heat rather than heatwave duration in CEU, they have equivalent influences on both in MED. Overall, the impacts of greenhouse gases dominate the intensification of heatwave duration at a regional scale, while the cooling effects of anthropogenic aerosols on cumulative heat are more influential in Europe, Asia, and North America. With significant efforts in global emission reduction, whether decreases in co-emitted aerosols contribute to heatwave intensification requires further investigation.

3.3. Diminishing Influence of Reduced Anthropogenic Aerosols on Heatwaves

We examine how trends in heatwave duration and cumulative heat have evolved since the pre-industrial period. For cumulative heat, the historical decadal trend shows evident acceleration during the industrial era. Globally, the increase rate of the cumulative heat in historical simulations is lower than under GHG-only conditions. However, the accelerations in historical simulations exceed those from GHG-only forcings after the 1970s (Figure 3a). This feature is also observed in the duration of heatwave events (Figure S4a in Supporting Information S1). Meanwhile, the decadal trends under AA-only conditions shift from negative to positive values after the 1970s, indicating a gradually diminishing negative effect of anthropogenic aerosols. Regionally, the increasing trends of cumulative heat in CNA, ENA, CEU, and CAS are much faster in recent decades, exceeding those under GHG-only conditions (Figure 3b). Trends under AA-only conditions in these regions show a shift toward positive effects. In comparison, heatwave duration shows a faster increase in AMZ and NEB (Figure S4 in Supporting Information S1). These results indicate that the combined anthropogenic influence on heatwaves lead to accelerated intensification, exceeding the rate of greenhouse gas-only forcings. Although a deceleration in heatwave trends is seen under GHG-only conditions, the weakening effects of anthropogenic aerosols contribute to the persistent acceleration of heatwaves on both global and regional scales. From the pre-industrial period, historical heatwave duration trends continuously accelerate and exceed those under GHG-only conditions (Figures S5a and S5d in Supporting Information S1). In comparison, NAT-only simulations show a few changes in heatwave duration trends (Figures S5e and S5f in Supporting Information S1). The weakening effects of anthropogenic aerosols are evident, however, regions like North America, Europe, and North Africa shift to the intensification from the 1990s onward (Figures S5g and S5h in Supporting Information S1). Changes in cumulative heat are more significant with divergent evolutions in GHG-only and AA-only conditions (Figure S6 in Supporting Information S1). In recent decades, heatwave trends driven by greenhouse gas forcing show extensive deceleration, while the shift in trends from anthropogenic aerosol simulations are more concentrated in the mid-latitudes in the Northern Hemisphere (Figures S6d and S6h in Supporting Information S1). This suggests that the combined effects of human-induced climate changes on heatwaves have significant regional discrepancy.

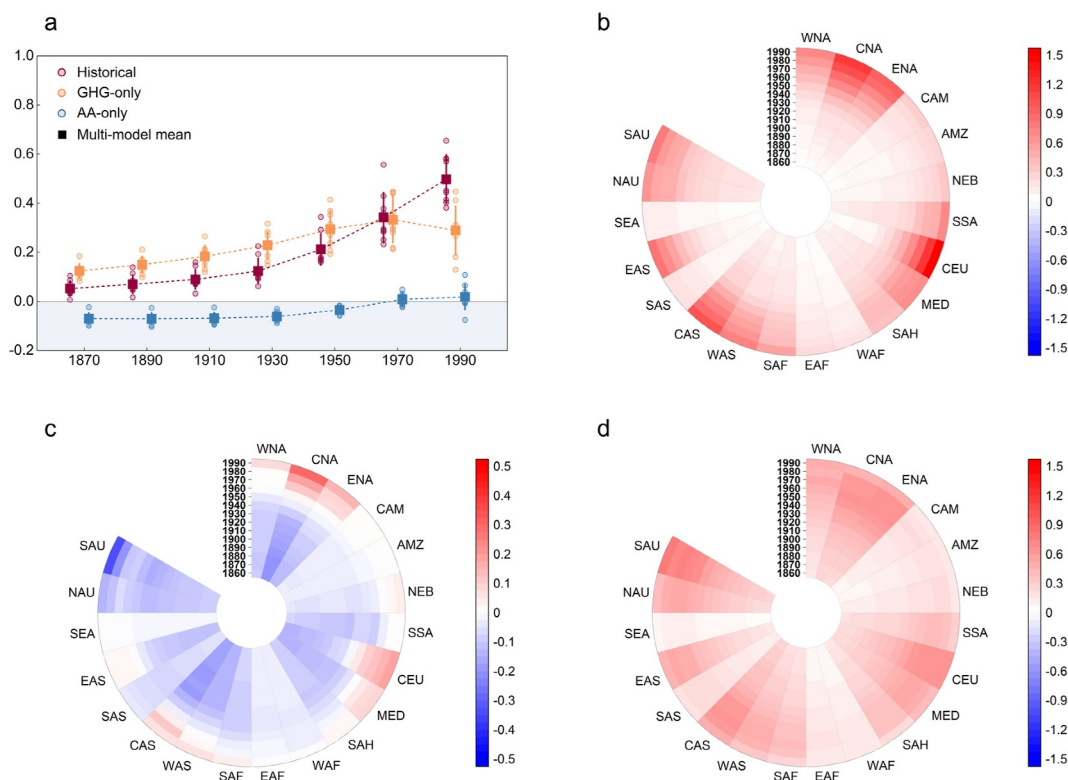


Figure 3. Evolution of decadal trends in the daily average cumulative heat in extreme heatwave events. (a) Global mean trends of the daily average cumulative heat driven by historical, greenhouse gas-only and anthropogenic aerosol-only forcings, commencing from 1851 to 1990. The boxes indicate the multi-model mean trends with an interval of 20 years from 1870. The colored dots indicate each climate model values. All trends truncate in 2019. (b) Decadal trends in the daily average cumulative heat under the historical condition. (c) Same as (b) but for the anthropogenic aerosol-only condition. (d) Same as (b) but for the greenhouse gas-only condition. Decadal trends are identified at each grid cell for each ensemble and then averaged over the IPCC SREX regions.

We further examine changes in heatwave characteristics driven by anthropogenic forcings at regional scales using Probability Ratio (PR) framework. The PR of cumulative heat and heatwave durations is calculated at the grid cell level and then averaged over IPCC SREX regions. The cumulative heat trends under GHG-only and AA-only conditions show inter-regional variability relative to historical forcings (Figure 4). From the pre-industrial period, cumulative heat trends under GHG-only forcing are faster than historical forcing in most regions, indicating a dominant role of greenhouse gases in intensifying heat risks. However, there is a rapid reduction, decreasing to less than 1 after the 1970s in boreal regions, especially in CEU and EAS. The weakening effects of anthropogenic aerosol also show a large reduction, approaching no changes after the 1970s. In CNA, ENA, MED, CEU and CAS, it shifts from negative to positive values, contributing to cumulative heat intensification with greenhouse gas forcings. In contrast, the anthropogenic aerosols have a cooling effect in SAU, but the trends driven by greenhouse gases are intensifying faster than historical conditions until recent decades. For the duration of heatwave events, the trend ratio of AA-only conditions relative to historical conditions is much smaller than those of GHG-only conditions, indicating that anthropogenic aerosols have little impact on heatwave duration in most regions (Figure S7 in Supporting Information S1). In recent decades, the trend ratio attributable to greenhouse gases alone has declined to approximately unity, maintaining a parallel rate of increase relative to historical baseline conditions. These findings demonstrate that greenhouse gases primarily drive the prolongation of heatwave duration, whereas anthropogenic aerosols exert a more pronounced influence on the cumulative thermal intensity during heatwave episodes. The accelerated reduction in the mitigating effects of anthropogenic aerosols has resulted in the intensification of regional heatwave events. The combined influence of individual anthropogenic forcing agents and the regional equilibrium between greenhouse gas warming and aerosol cooling collectively modulate heatwave dynamics since the pre-industrial era.

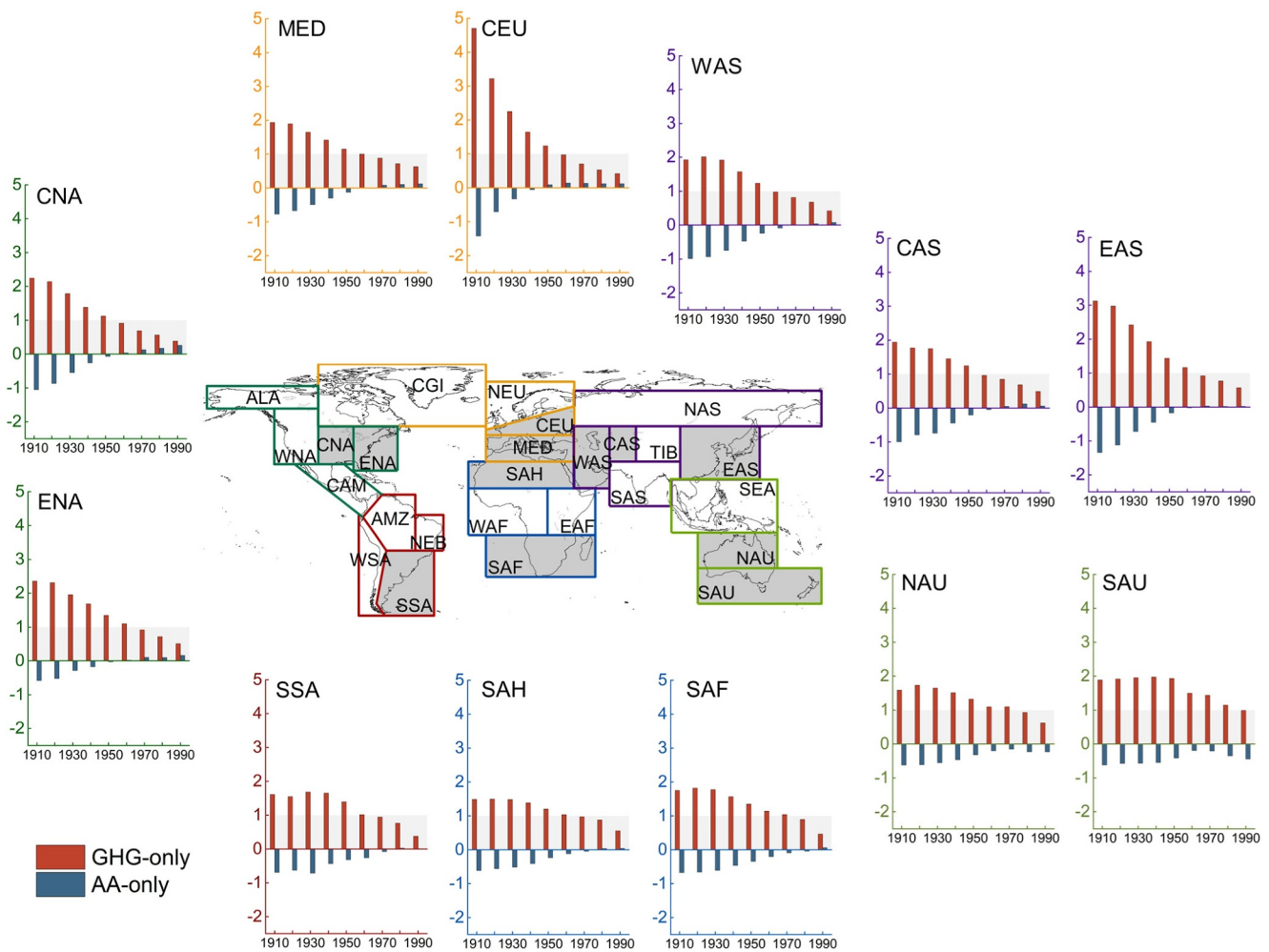


Figure 4. Probability Ratio (PR) of the daily average cumulative heat trend for greenhouse gas-only (GHG-only) and anthropogenic aerosol-only (AA-only) conditions. Values above 1 indicate accelerated intensification in daily average cumulative heat and values below 1 indicate retardatory changes. Negative values indicate diminution in daily average cumulative heat of heatwave events. The attributable changes in the trend of daily average cumulative heat under GHG-only and AA-only conditions relative to historical simulations are indicated with yellow and blue histograms, respectively. PR_{trend} is identified at each grid cell and then are averaged over the IPCC SREX regions.

4. Discussion and Summary

Using CMIP6 historical simulations along with the DAMIP and ScenarioMIP SSP2-4.5 scenarios, we provide a global assessment of the impacts of human-induced climate change on the duration and cumulative heat of extreme heatwaves since the pre-industrial period. Compared to the pre-industrial period (pre-1880s), the intensification of heatwave duration and cumulative heat in the last 3 decades (post-1990s) has increased by factors 5.12 and 1.76 times, respectively. The contributions of individual anthropogenic and natural forcings to heatwave evolutions are assessed using GHG-only, AA-only, and NAT-only simulations. Globally, heatwave duration and cumulative heat driven by GHG-only forcings increased by $+2.77 \pm 0.85$ (days) and $+1.76 \pm 0.31$ ($^{\circ}\text{C}^2$) during 1990–2019 relative to 1851–1880, while AA-only forcings showed decreases of -1.10 ± 0.34 (days) and -0.85 ± 0.14 ($^{\circ}\text{C}^2$). Previous attribution studies have used model simulations to examine the contributions of anthropogenic climate change to global mean temperature (Easterling et al., 2016; Fischer & Knutti, 2014, 2015; Wang et al., 2020). These studies have shown that temperature changes ranging from 1.2 to 1.9 $^{\circ}\text{C}$ can be attributed to greenhouse gases, while aerosols have contributed to changes between -0.7 and 0.1°C , respectively, when comparing the periods of 2010–2019 to 1850–1990. In this study, the positive effects of greenhouse gases on heatwave duration are more than twice the weakening effects of anthropogenic aerosols, while anthropogenic

aerosols are more influential on cumulative heat than heatwave duration. For NAT-only forcings, minimal impacts are observed on heatwave duration and heat anomalies, indicating a consistently negligible contribution from NAT-only simulations to temperature changes (Gillett et al., 2021). Importantly, acceleration in heatwave intensification during past decades has exceeded those driven by greenhouse gases. Although the impacts of greenhouse gases on heatwave increases are diminishing, the declining influence of anthropogenic aerosols, which now even tend to exacerbate heatwaves, contributes to the acceleration in extreme heat events. By examining the evolution of heatwaves under individual anthropogenic forcings, we demonstrate how historical shifts in heatwave characteristics are contingent upon regional balances between the effects of anthropogenic greenhouse gases and aerosols.

Since the establishment of the IPCC, the development of emission reduction policies aims to limit the impacts of anthropogenic activities on global climate change. From the UNFCCC in 1992 to the Paris Agreement's target in 2015, the emission reduction development shifts from unilateral action by developed countries to universal global participation, systematically advancing global progress toward carbon neutrality objectives. During the 21st Conference of UNFCCC in Paris, the Paris Agreement was established to enhance the global response to the climate change threat, promoting sustainable development (UNFCCC, 2015). Recent studies have demonstrated that meeting the Paris Agreement targets for global greenhouse gas emissions alone is inadequate to mitigate climate risks, highlighting the need for more immediate and substantial emission reductions (Schleussner et al., 2024). Monthly spatial patterns show that aerosols distribute more extensively and concentrate in extended summer seasons. Globally, the aerosols have a higher concentration in Africa, western and southern Asia and Eastern Asia. During recent 2 decades, the aerosols show decreases in Europe, North America, East Africa and Australia and SEA (Figures S8 and S9 in Supporting Information S1). These regions not only experienced significant increases in extreme heatwaves but also shifted effects of diminishing aerosols on heatwaves. Meanwhile, significant decreasing trends of aerosols exhibits in ALA, CEU, CNA, ENA, MED, NAS and NEU, which dominated the evolution of regional aerosol variations (Figure S10 in Supporting Information S1). The decreases in regional aerosol further aggravate the intensification of extreme heatwaves. However, decreases in co-emitted cooling aerosols inadvertently exacerbate the cumulative heat of extreme heatwaves. For instance, reducing anthropogenic aerosols will lead to greater increases in wildfire activity in the Northern Hemisphere boreal forests compared to scenarios without climate policy and significant rises in greenhouse gases (Allen et al., 2024). In this study, affected by the declining effects of anthropogenic aerosols, the decadal trends in heatwave duration and cumulative heat driven by historical forcings show 1.07 ± 0.32 (days) decade⁻¹ and 0.47 ± 0.09 (°C²) decade⁻¹ in the last 3 decades (1990–2019), exceeding those of greenhouse gas simulations of 0.83 ± 0.35 (days) decade⁻¹ and 0.28 ± 0.09 (°C²) decade⁻¹, respectively. PR analyses suggest that CNA, ENA and CEU have higher risks of heat exposure during heatwave events. Conversely, the opposite effects of anthropogenic aerosols in NAU and SAU have persisted in recent decades.

We further investigate the underlying mechanism of human-induced forcings driven by changes of anthropogenic aerosols. Changes in total cloud cover percentage show that AA-induced cloud cover decreased in recent decades in CNA, CEU, and NAU (Figures 5a and 5b), which further increased surface shortwave radiation in these regions (Figures 6a and 6b). These results demonstrated the weakening effects of aerosols on regional heatwave intensification. Decadal trends in cloud cover driven by AA-only conditions show accelerated reduction in CNA and CEU after global climate policy (Figures 5c and 5d), along with the accelerated increase in surface shortwave radiation. Although weakening effects of AA are also exhibited in MED and CAS, changes in cloud cover in these regions are dominated by the GHG-only forcing (Figures 5e and 5f), which also dominate the cloud changes in NAU and SAU, further intensifying regional heatwaves (Figures 5g and 5h). These physical mechanism analyses indicate that CNA and CEU will experience sustained cloud cover decrease and shortwave flux increases, leading to higher risks of heat exposure with current climate policy.

Anthropogenic contributions to regional heatwaves have been confirmed worldwide (Bercos-Hickey et al., 2022; Faranda et al., 2023), prompting more studies to investigate the role of human-induced climate change in amplifying heatwave intensification or temperature increase (Luo et al., 2024; Mukherjee et al., 2022). While the significant influence of greenhouse gases on temperature increases is acknowledged, the second largest climate forcing factor, aerosols, which have crucial impacts on climate over the industrial era, have received little attention under current climate mitigation policies. Our study provides a comprehensive

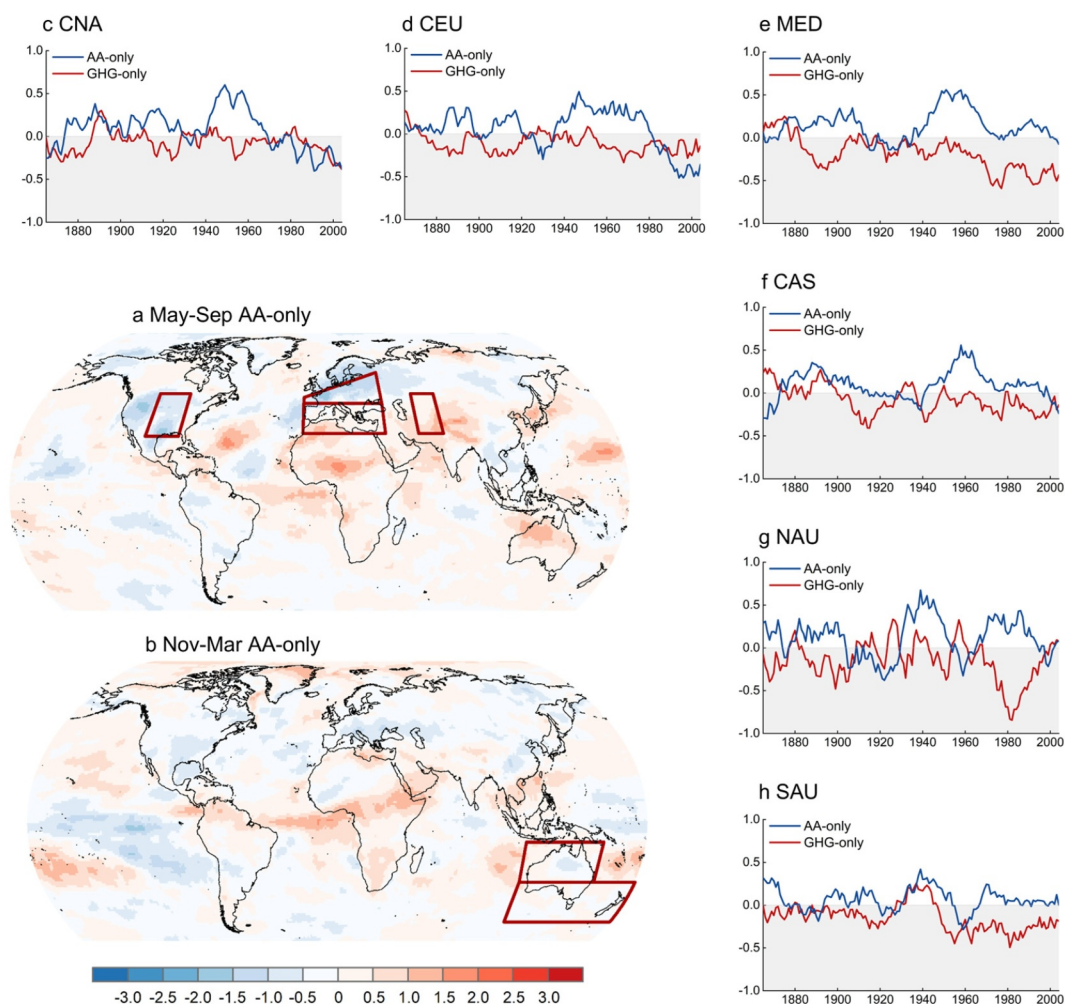


Figure 5. Total cloud cover changes driven by the anthropogenic conditions. (a) Global patterns of differences in the cloud cover (May–Sep) between the 1990–2019 and pre-three decades; (b) same as (a) but for the warm spell of Southern Hemisphere (Nov–Mar); (c) Decadal trends of the cloud cover in central North America (CNA) driven by the AA-only and GHG-only forcings; (d) same as (c) but for central Europe (CEU); (e) same as (c) but for south Europe/Mediterranean (MED); (f) same as (c) but for central Asia (CAS); (g) same as (c) but for north Australia (NAU); (h) same as (c) but for Newland/south Australis (SAU). All trends are calculated with a 30-year window from 1851 to 2019. The x-axis denotes the 15th year of each window.

assessment of the impacts of anthropogenic greenhouse gases and aerosols on heatwave evolutions at global and regional scales. Exploring heatwave changes from the pre-industrial period rather than recent warming decades is useful in advancing our understanding of human contributions to observed heatwave intensification. Compared with natural forcings, anthropogenic forcings exhibit significant but divergent impacts on heatwave intensification across the globe. The impacts of greenhouse gases contribute more to heatwave duration than cumulative heat, while anthropogenic aerosols are more influential in reducing the cumulative heat of heatwave events. Importantly, the well-known aggravated effects of greenhouse gases show deceleration at both global and regional scales. On the other hand, the cooling effects of anthropogenic aerosols show rapid weakening and even shift to positive effects in SREX regions. Global emission reduction efforts regarding the goals of the Paris Agreement aim to decline long-term climate risks, however, the consequence of mitigation inadvertently reverses the intended goals, which have large spatial heterogeneity. Our study provides a global-scale assessment of how diminished aerosol cooling unveils previously concealed warming trends, driving heatwave intensification and necessitating integrated risk management frameworks for vulnerable infrastructure and

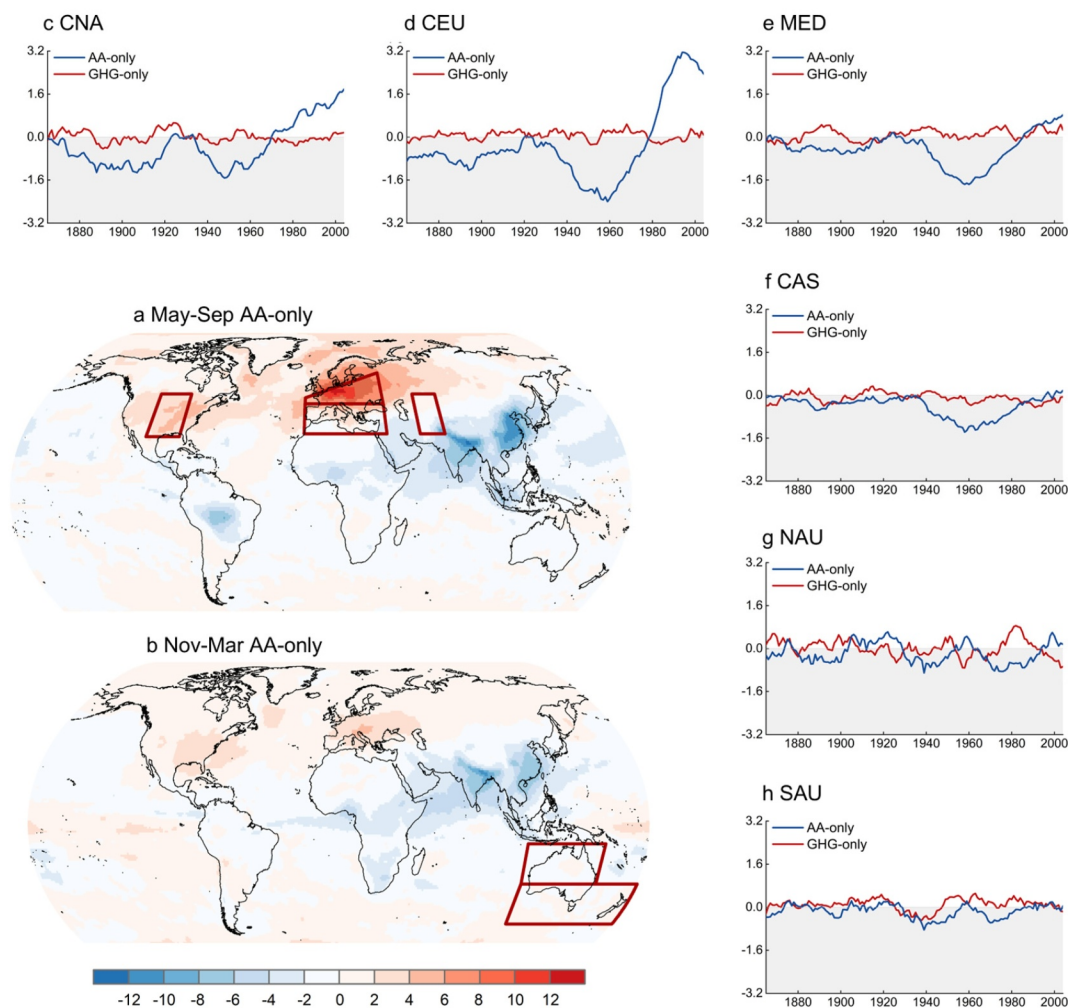


Figure 6. Surface shortwave radiation changes driven by the anthropogenic conditions. (a) Global patterns of differences in the surface shortwave radiation (May–Sep) between the 1990–2019 and pre-three decades; (b), same as (a) but for the warm spell of Southern Hemisphere (Nov–Mar); (c), decadal trends of the surface shortwave radiation in central North America (CNA) driven by the AA-only and GHG-only forcings; (d), same as (c) but for central Europe (CEU); (e), same as (c) but for south Europe/Mediterranean (MED); (f) same as (c) but for central Asia (CAS); (g) same as (c) but for north Australia (NAU); (h) same as (c) but for Newland/south Australis (SAU). All trends are calculated with a 30-year window from 1851 to 2019. The x -axis denotes the 15th year of each window.

population systems across diverse geographical contexts. Given the devastating impacts of extreme heatwave on human health and ecosystem sustainability, it is imperative to understand the limitation of implementation and interventions of global climate policies.

Conflict of Interest

The authors declare no conflicts of interest relevant to this study.

Data Availability Statement

Daily maximum and minimum temperatures are available from CMIP6 climate models (Gillett et al., 2016). The temperature data sets from the MERRA2, JRA55, ERA5 and NCEP/NCAR are available via GMAO (2015), Kobayashi et al. (2015), Hersbash et al. (2023), Kalnay et al. (1996), respectively. Monthly total cloud cover

percentage and surface shortwave flux of CMIP6 historical, DAMIP and ScenarioMIP simulations are available via Gillett et al., 2016. The scripts used to analyze data in this study are available via Wei (2025).

Acknowledgments

This work was jointly supported by the National Key R&D Program of China (2024YFF1307101), the National Natural Science Foundation of China (U2240218, 42307117, 52479010), China Postdoctoral Science Foundation (2023M740984) and Hong Kong Scholars Program (XJ2024046). We acknowledge the World Climate Research Program's Working Group on Coupled Modeling, which is responsible for the Coupled Model Intercomparison Project (CMIP), and we thank the climate modeling groups for producing and making available their model output.

References

- Allen, C. D., Breshears, D. D., & McDowell, N. G. (2015). On underestimation of global vulnerability to tree mortality and forest die-off from hotter drought in the Anthropocene. *Ecosphere*, 6(8), 1–55. <https://doi.org/10.1890/ES15-00203.1>
- Allen, R. J., Samsel, B. H., Wilcox, L. J. F. R. A., & Fisher, R. A. (2024). Are Northern Hemisphere boreal forest fires more sensitive to future aerosol mitigation than to greenhouse gas-driven warming? *Science Advances*, 10(13), ead14007. <https://doi.org/10.1126/sciadv.ad14007>
- Åström, D. O., Forsberg, B., Ebi, K. L., & Rocklöv, J. (2013). Attributing mortality from extreme temperatures to climate change in Stockholm, Sweden. *Nature Climate Change*, 3(12), 1050–1054. <https://doi.org/10.1038/nclimate2022>
- Barkhordarian, A. (2024). Disentangling regional climate change: Assessing the contribution of global- and regional-scale anthropogenic factors to observed regional warming. *Environmental Research Letters*, 19(12), 124045. <https://doi.org/10.1088/1748-9326/ad8f49>
- Bellouin, N., Quaas, J., Gryspeerdt, E., Kinne, S., Stier, P., Watson-Paris, D., et al. (2020). Bounding global aerosol radiative forcing of climate change. *Reviews of Geophysics*, 58(1), e2019RG000660. <https://doi.org/10.1029/2019RG000660>
- Bercos-Hickey, E., O'Brien, T. A., Wehner, M. F., Zhang, L., Patricola, C. M., Huang, H., & Risser, M. D. (2022). Anthropogenic contributions to the 2021 Pacific Northwest heatwave. *Geophysical Research Letters*, 49(23), e2022GL099396. <https://doi.org/10.1029/2022gl099396>
- Bras, T. A., Seixas, J., Carvalhais, N., Brás, T. A., Seixas, J., & Jägermeyr, J. (2021). Severity of drought and heatwave crop losses tripled over the last five decades in Europe. *Environmental Research Letters*, 16(6), 065012. <https://doi.org/10.1088/1748-9326/abf004>
- Chemke, R., & Yuval, J. (2023). Human-induced weakening of the Northern Hemisphere tropical circulation. *Nature*, 617(7961), 529–532. <https://doi.org/10.1038/s41586-023-05903-1>
- Ciais, P., Reichstein, M., Viovy, N., Granier, A., Ogee, J., Allard, V., et al. (2005). Europe-wide reduction in primary productivity caused by the heat and drought in 2003. *Nature*, 437(7058), 529–533. <https://doi.org/10.1038/nature03972>
- Diffenbaugh, N. S., Singh, D., Mankin, J. S., Diffenbaugh, N. S., Mankin, J. S., Horton, D. E., et al. (2017). Quantifying the influence of global warming on unprecedented extreme climate events. *Proceedings of the National Academy of Sciences of the United States of America*, 114(19), 4881–4886. <https://doi.org/10.1073/pnas.1618082114>
- Easterling, D. R., Kunkel, K. E., Wehner, M. F., & Sun, L. (2016). Detection and attribution of climate extremes in the observed record. *Weather and Climate Extremes*, 11, 17–27. <https://doi.org/10.1016/j.wace.2016.01.001>
- Eyring, V., Bony, S., Meehl, G. A., Senior, C. A., Stevens, B., Stouffer, R. J., & Taylor, K. E. (2016). Overview of the Coupled Model Intercomparison Project Phase 6 (CMIP6) experimental design and organization. *Geoscientific Model Development*, 9(5), 1937–1958. <https://doi.org/10.5194/gmd-9-1937-2016>
- Faranda, D., Messori, G., Jezequel, A., Vrac, M., & Yiou, P. (2023). Atmospheric circulation compounds anthropogenic warming and impacts of climate extremes in Europe. *Proceedings of the National Academy of Sciences of the United States of America*, 120(13), e2214525120. <https://doi.org/10.1073/pnas.2214525120>
- Fischer, E. M., & Knutti, R. (2014). Detection of spatially aggregated changes in temperature and precipitation extremes. *Geophysical Research Letters*, 41(2), 547–554. <https://doi.org/10.1002/2013GL058499>
- Fischer, E. M., & Knutti, R. (2015). Anthropogenic contribution to global occurrence of heavy-precipitation and high-temperature extremes. *Nature Climate Change*, 5(6), 560–564. <https://doi.org/10.1038/nclimate2617>
- Fischer, E. M., & Schär, C. (2010). Consistent geographical patterns of changes in high-impact European heatwaves. *Nature Geoscience*, 3(6), 398–403. <https://doi.org/10.1038/ngeo866>
- Gillett, N. P., Kirchmeier-Young, M., Ribes, A., Shiogama, H., Hegerl, G. C., Knutti, R., et al. (2021). Constraining human contributions to observed warming since the pre-industrial period. *Nature Climate Change*, 11(3), 207–212. <https://doi.org/10.1038/s41558-020-00965-9>
- Gillett, N. P., Shiogama, H., Funke, B., Hegerl, G., Knutti, R., Matthes, K., et al. (2016). The Detection and Attribution Model Intercomparison Project (DAMIP v1.0) contribution to CMIP6. *Geoscientific Model Development*, 9(10), 3685–3697. <https://doi.org/10.5194/gmd-9-3685-2016>
- Global Modeling and Assimilation Office (GMAO) (2015). MERRA-2 statD_2d_slv_Nx: 2d, daily, aggregated statistics, single-level, assimilation, single-level diagnostics V5.12.4, Greenbelt, MD, USA, Goddard Earth Sciences Data and Information Services Center (GES DISC). Accessed: [Data Access Date], <https://doi.org/10.5067/9SC1VNTGWVW3>
- Grant, L., Vanderkelen, I., Gudmundsson, L., Tan, Z., Perroud, M., Stepanenko, V. M., et al. (2021). Attribution of global lake systems change to anthropogenic forcing. *Nature Geoscience*, 14(11), 849–854. <https://doi.org/10.1038/s41561-021-00833-x>
- Guo, Y., Gasparrini, A., Li, S., Sera, F., Vicedo-Cabrera, A. M., de Sousa Zanotti Stagliorio Coelho, M., et al. (2018). Quantifying excess deaths related to heat waves under climate change scenarios: A multicountry time series modelling study. *PLoS Medicine*, 15(7), e1002629. <https://doi.org/10.1371/journal.pmed.1002629>
- Hersbach, H., Bell, B., Berrisford, P., Biavati, G., Horányi, A., Muñoz Sabater, J., et al. (2023). ERA5 hourly data on pressure levels from 1940 to present [Dataset]. <https://cds.climate.copernicus.eu/datasets/reanalysis-era5-pressure-levels?tab=download>
- Jiang, J., Zhou, T., Qian, Y., Li, C., Song, F., Li, H., et al. (2023). Precipitation regime changes in High Mountain Asia driven by cleaner air. *Nature*, 623(7987), 544–549. <https://doi.org/10.1038/s41586-023-06619-y>
- Kalnay, E., Kanamitsu, M., Kistler, R., Collins, W., Deaven, D., Gandin, L., et al. (1996). The NCEP/NCAR 40-year reanalysis project. *Bulletin of the American Meteorological Society*, 77, 437–470. Retrieved from <https://psl.noaa.gov/data/gridded/data.ncep.reanalysis.html>
- Kim, Y., Min, S., Tung, Y., Kim, Y.-H., Min, S.-K., Zhang, X., et al. (2016). Attribution of extreme temperature changes during 1951–2010. *Climate Dynamics*, 46(5–6), 1769–1782. <https://doi.org/10.1007/s00382-015-2674-2>
- Kobayashi, S., Ota, Y., Harada, H., Ebata, A., Moriya, M., Onoda, H., et al. (2015). The JRA-55 reanalysis: General specifications and basic characteristics. *Journal of the Meteorological Society of Japan*, 93(1), 5–48. <https://doi.org/10.2151/jmsj.2015-001>
- Li, Z., Lau, W., Ramanathan, V., Wu, G., Ding, Y., Manoj, M. G., et al. (2016). Aerosol and monsoon climate interactions over Asia. *Reviews of Geophysics*, 54(4), 866–929. <https://doi.org/10.1002/2015RG000500>
- Lobell, D. B., & Field, C. B. (2007). Global scale climate–crop yield relationships and the impacts of recent warming. *Environmental Research Letters*, 2(1), 014002. <https://doi.org/10.1088/1748-9326/2/1/014002>
- Luo, M., Wu, S., Lau, G., Pei, T., Liu, Z., Wang, X., et al. (2024). Anthropogenic forcing has increased the risk of longer-traveling and slower-moving large contiguous heatwaves. *Science Advances*, 10(13). <https://doi.org/10.1126/sciadv.ad11598>
- Marotzke, J., & Forster, P. M. (2015). Forcing, feedback and internal variability in global temperature trends. *Nature*, 517(7536), 565–570. <https://doi.org/10.1038/nature14117>

- Marvel, K., Cook, B. I., Bonfils, C. J. W., Durack, P. J., Smerdon, J. E., & Williams, A. P. (2019). Twentieth-century hydroclimate changes consistent with human influence. *Nature*, *569*(7754), 59–65. <https://doi.org/10.1038/s41586-019-1149-8>
- Meinshausen, M., Meinshausen, N., Hare, W., Raper, S. C. B., Frieler, K., Thorne, J., et al. (2009). Greenhouse-gas emission targets for limiting global warming to 2°C. *Nature*, *458*(7242), 1158–1162. <https://doi.org/10.1038/nature08017>
- Mhawish, A., Sarangi, C., Babu, P., Kumar, M., Bilal, M., & Qiu, Z. (2022). Observational evidence of elevated smoke layers during crop residue burning season over Delhi: Potential implications on associated heterogeneous PM_{2.5} enhancements. *Remote Sensing of Environment*, *280*, 113167. <https://doi.org/10.1016/j.rse.2022.113167>
- Mukherjee, S., Mishra, A., Mishra, M., & Kao, S. C. (2022). Relative effect of anthropogenic warming and natural climate variability to changes in Compound drought and heatwaves. *Journal of Hydrology*, *605*, 127396. <https://doi.org/10.1016/j.jhydrol.2021.127396>
- Mukherjee, S., & Mishra, A. K. (2021). Increase in compound drought and heatwaves in a warming World. *Geophysical Research Letters*, *48*(1). <https://doi.org/10.1029/2020GL090617>
- Nair, H. R. C. R., Budhavant, K., Manoj, M. R., Andersson, A., Satheesh, S. K., Ramanathan, V., & Gustafsson, Ö. (2023). Aerosol demasking enhances climate warming over South Asia. *npj Climate and Atmospheric Science*, *6*(1), 39. <https://doi.org/10.1038/s41612-023-00367-6>
- Nairn, J., Ostendorf, B., & Bi, P. (2018). Performance of excess heat factor severity as a global heatwave health impact index. *International Journal of Environmental Research and Public Health*, *15*(11), 2494. <https://doi.org/10.3390/ijerph15112494>
- Nairn, J. R., & Fawcett, R., & Australia. Bureau of Meteorology & Centre for Australian Weather and Climate Re, & search, issuing body & CSIRO. (2013). Defining heatwaves: Heatwave defined as a heat-impact event servicing all community and business sectors in Australia. Retrieved from <http://nla.gov.au/nla.obj-2968723484>
- Nairn, J. R., & Fawcett, R. J. B. (2015). The excess heat factor: A metric for heatwave intensity and its use in classifying heatwave severity. *International Journal of Environmental Research and Public Health*, *12*(1), 227–253. <https://doi.org/10.3390/ijerph120100227>
- O'Neill, B. C., Tebaldi, C., van Vuuren, D. P., Eyring, V., Friedlingstein, P., Hurtt, G., et al. (2016). The Scenario Model Intercomparison Project (ScenarioMIP) for CMIP6. *Geoscientific Model Development*, *9*, 3461–3482. <https://doi.org/10.5194/gmd-9-3461-2016>
- Padrón, R. S., Gudmundsson, L., Decharme, B., Ducharme, A., Lawrence, D. M., Mao, J., et al. (2020). Observed changes in dry-season water availability attributed to human-induced climate change. *Nature Geoscience*, *13*(7), 477–481. <https://doi.org/10.1038/s41561-020-0594-1>
- Perkins, S. E., Alexander, L. V., & Nairn, J. R. (2012). Increasing frequency, intensity and duration of observed global heatwaves and warm spells. *Geophysical Research Letters*, *39*(20), L20714. <https://doi.org/10.1029/2012GL053361>
- Perkins, S. E., Argüeso, D., & White, C. J. (2015). Relationships between climate variability, soil moisture, and Australian heatwaves. *Journal of Geophysical Research: Atmospheres*, *120*(16), 8144–8164. <https://doi.org/10.1002/2015JD023592>
- Perkins-Kirkpatrick, S. E., & Lewis, S. C. (2020). Increasing trends in regional heatwaves. *Nature Communications*, *11*(1), 3357. <https://doi.org/10.1038/s41467-020-16970-7>
- Persad, G. G., & Caldeira, K. (2018). Divergent global-scale temperature effects from identical aerosols emitted in different regions. *Nature Communications*, *9*(1), 3289. <https://doi.org/10.1038/s41467-018-05838-6>
- Russo, S., Sillmann, J., Fischer, E. M., & Fischer, E. M. (2015). Top ten European heatwaves since 1950 and their occurrence in the coming decades. *Environmental Research Letters: ERL*, *10*(12), 124003. <https://doi.org/10.1088/1748-9326/10/12/124003>
- Schleussner, C. F., Ganti, G., Lejeune, Q., Zhu, B., Pfeleiderer, P., Prütz, R., et al. (2024). Overconfidence in climate overshoot. *Nature*, *634*(8033), 366–373. <https://doi.org/10.1038/s41586-024-08020-9>
- Schurer, A. P., Mann, M. E., Hawkins, E., Tett, S. F. B., & Hegerl, G. C. (2017). Importance of the pre-industrial baseline for likelihood of exceeding Paris goals. *Nature Climate Change*, *7*(8), 563–567. <https://doi.org/10.1038/nclimate3345>
- Sharma, S., & Mujumdar, P. (2017). Increasing frequency and spatial extent of concurrent meteorological droughts and heatwaves in India. *Scientific Reports*, *7*(1), 15582. <https://doi.org/10.1038/s41598-017-15896-3>
- Smale, D. A., Wernberg, T., Oliver, E. C. J., Thomsen, M., Harvey, B. P., Straub, S. C., et al. (2019). Marine heatwaves threaten global biodiversity and the provision of ecosystem services. *Nature Climate Change*, *9*(4), 306–312. <https://doi.org/10.1038/s41558-019-0412-1>
- Stott, P. A., Stone, D. A., & Allen, M. R. (2004). Human contribution to the European heatwave of 2003. *Nature*, *432*(7017), 610–614. <https://doi.org/10.1038/nature03089>
- Tan, X., Wu, X., Huang, Z., Fu, J., Tan, X., Deng, S., et al. (2023). Increasing global precipitation whiplash due to anthropogenic greenhouse gas emissions. *Nature Communications*, *14*(1), 2796. <https://doi.org/10.1038/s41467-023-38510-9>
- Tang, S., Qiao, S., Wang, B., Liu, F., Feng, T., Yang, J., et al. (2023). Linkages of unprecedented 2022 Yangtze River valley heatwaves to Pakistan flood and triple-dip La Niña. *Npj Climate and Atmospheric Science*, *6*(1), 44. <https://doi.org/10.1038/s41612-023-00386-3>
- Teuling, A. J. (2018). A hot future for European droughts. *Nature Climate Change*, *8*(5), 364–365. <https://doi.org/10.1038/s41558-018-0154-5>
- Teuling, A. J., Seneviratne, S. I., Stöckli, R., Reichstein, M., Moors, E., Ciais, P., et al. (2010). Contrasting response of European forest and grassland energy exchange to heatwaves. *Nature Geoscience*, *3*(10), 722–727. <https://doi.org/10.1038/ngeo950>
- Thiery, W., Visser, A. J., Fischer, E. M., Hauser, M., Seneviratne, S. I., Lawrence, D. M., et al. (2020). Warming of hot extremes alleviated by expanding irrigation. *Nature Communications*, *11*(1), 290. <https://doi.org/10.1038/s41467-019-14075-4>
- Tripathy, K. P., & Mishra, A. K. (2023). How unusual is the 2022 European compound drought and heatwave event? *Geophysical Research Letters*, *50*(15). <https://doi.org/10.1029/2023GL105453>
- UNFCCC. (2015). Adoption of the Paris agreement, FCCC/CP/2015/L.9/Rev.1. *United Nations Framework Convention on Climate Change*. Retrieved from <https://unfccc.int/resource/docs/2015/cop21/eng/l09r01.pdf>
- van der Wiel, K., & Bintanja, R. (2021). Contribution of climatic changes in mean and variability to monthly temperature and precipitation extremes. *Communications Earth & Environment*, *2*, 1. <https://doi.org/10.1038/s43247-020-00077-4>
- Wang, J., Chen, Y., Tett, S. F. B., Yan, Z., Zhai, P., Feng, J., & Xia, J. (2020). Anthropogenically-driven increases in the risks of summertime compound hot extremes. *Nature Communications*, *11*(1), 528. <https://doi.org/10.1038/s41467-019-14233-8>
- Wang, Z., Lei, Y., Che, H., Wu, B., & Zhang, X. (2024). Aerosol forcing regulating recent decadal change of summer water vapor budget over the Tibetan Plateau. *Nature Communications*, *15*(1), 2233. <https://doi.org/10.1038/s41467-024-46635-8>
- Wei, J. (2025). Code for “reduced anthropogenic aerosols reveal increased heatwaves driven by climate warming” (version v1) [Software]. *Zenodo*. <https://doi.org/10.5281/zenodo.13982674>
- Wei, J., Han, W., Wang, W., Zhang, L., & Rajagopalan, B. (2023). Intensification of heatwaves in China in recent decades: Roles of climate modes. *npj Climate and Atmospheric Science*, *6*(1), 98. <https://doi.org/10.1038/s41612-023-00428-w>
- Wei, J., Wang, W., Shao, Q., Yu, Z., Chen, Z., Huang, Y., & Xing, W. (2020). Heat wave variations across China tied to global SST modes. *Journal of Geophysical Research: Atmospheres*, *125*(6), e2019JD031612. <https://doi.org/10.1029/2019JD031612>
- Wei, J., Wang, W., Wang, G., Cao, M., Yang, L., Zhang, S., et al. (2023b). Projecting the changes in multifaceted characteristics of heatwave events across China. *Earth's Future*, *11*(3), e2022EF003387. <https://doi.org/10.1029/2022EF003387>

- Westerling, A. L., Hidalgo, H. G., Cayan, D. R., & Swetnam, T. W. (2006). Warming and earlier spring increase Western U.S. forest wildfire activity. *Science*, *313*(5789), 940–943. <https://doi.org/10.1126/science.1128834>
- White, C., Hudson, D., & Alves, O. (2013). ENSO, the IOD and the intraseasonal prediction of heat extremes across Australia using POAMA-2. *Climate Dynamics*, *43*(7–8), 1791–1810. <https://doi.org/10.1007/s00382-013-2007-2>
- Wild, M., Gilgen, H., Roesch, A., Ohmura, A., Long, C. N., Dutton, E. G., et al. (2005). From dimming to brightening: Decadal changes in solar radiation at Earth's surface. *Science*, *308*(5723), 847–850. <https://doi.org/10.1126/science.1103215>
- Xu, Z., FitzGerald, G., Guo, Y., Jalaludin, B., & Tong, S. (2016). Impact of heatwave on mortality under different heatwave definitions: A systematic review and meta-analysis. *Environment International*, *89*(90), 193–203. <https://doi.org/10.1016/j.envint.2016.02.007>
- Zhang, Q., Meng, J., Quan, J., Gao, Y., Zhao, D., Chen, P., & He, H. (2012). Impact of aerosol composition on cloud condensation nuclei activity. *Atmospheric Chemistry and Physics*, *12*(8), 3783–3790. <https://doi.org/10.5194/acp-12-3783-2012>
- Zhang, X., Zhou, T., Zhang, W., Wang, Y., Liu, Q., Li, H., et al. (2023). Increased impact of heat domes on 2021-like heat extremes in North America under global warming. *Nature Communications*, *14*(1), 1690. <https://doi.org/10.1038/s41467-023-37309-y>
- Zhu, J., Wang, S., & Fischer, E. M. (2022). Increased occurrence of day–night hot extremes in a warming climate. *Climate Dynamics*, *59*(5–6), 1297–1307. <https://doi.org/10.1007/s00382-021-06038-7>